Electronic Supplementary Material (ESI) for Journal of Materials Chemistry A.

Supplementary Information

# Strong Anisotropic Hydrogels with Ion Transport Capability *via* Reswelling Contrast of Two Oriented Polymer Networks

*Wei Cui*, *Menghan Pi*, *Ruijie Zhu*, *Zetao Xiong*, and *Rong Ran**

## Table of contents

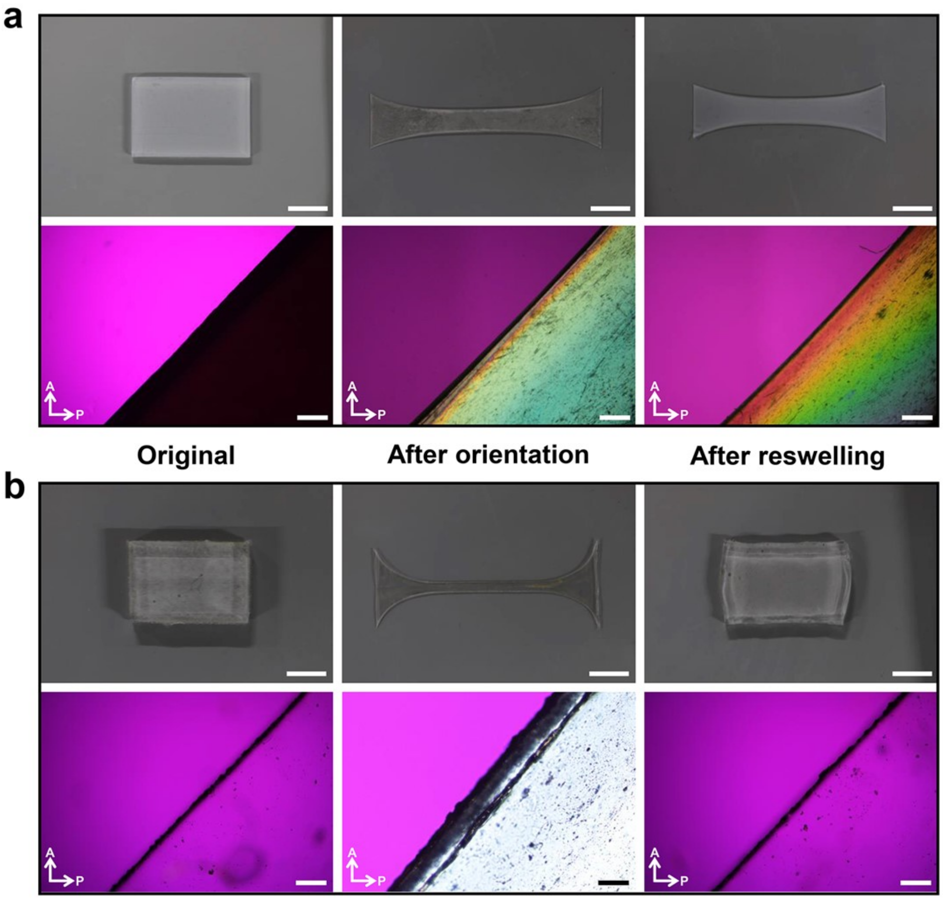

**Figure S1. The orienting-reswelling process of an individual $Ca^{2+}$-alginate and polyacrylamide hydrogel, respectively.** (a) Photographs and corresponding POM images of the orienting-reswelling process of the $Ca^{2+}$-alginate hydrogel. (b) Photographs and corresponding POM images of the orienting-reswelling process of the polyacrylamide hydrogel. Both the $Ca^{2+}$-alginate and polyacrylamide hydrogels show birefringence after orientation. However, their reswelling behaviors are in clear contrast. The $Ca^{2+}$-alginate gel maintains the orientation and anisotropic structure after reswelling, whereas the polyacrylamide hydrogel recovers its original shape and isotropy after reswelling. A: analyzer, P: polarizer. The scale bars in the photographs and POM images represent 10 mm and 200 μm, respectively.

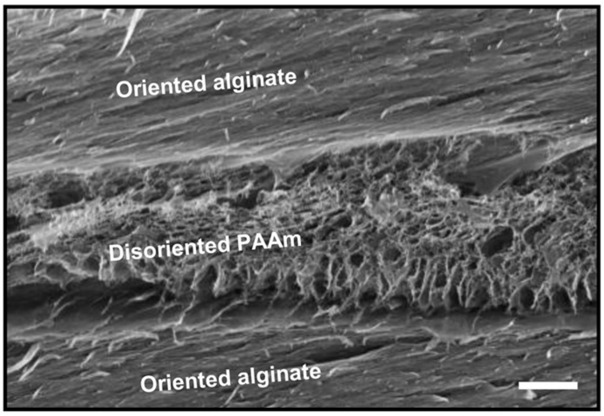

**Figure S2. A locally enlarged SEM image of Figure 1c-ii in the manuscript.** It shows that the PAAm chains disorient after reswelling, whereas the alginate chains maintain the orientation. Such a reswelling contrast leads to the heterogenous soft-stiff structure of the hybrid gel. The scale bar represents 2 μm.

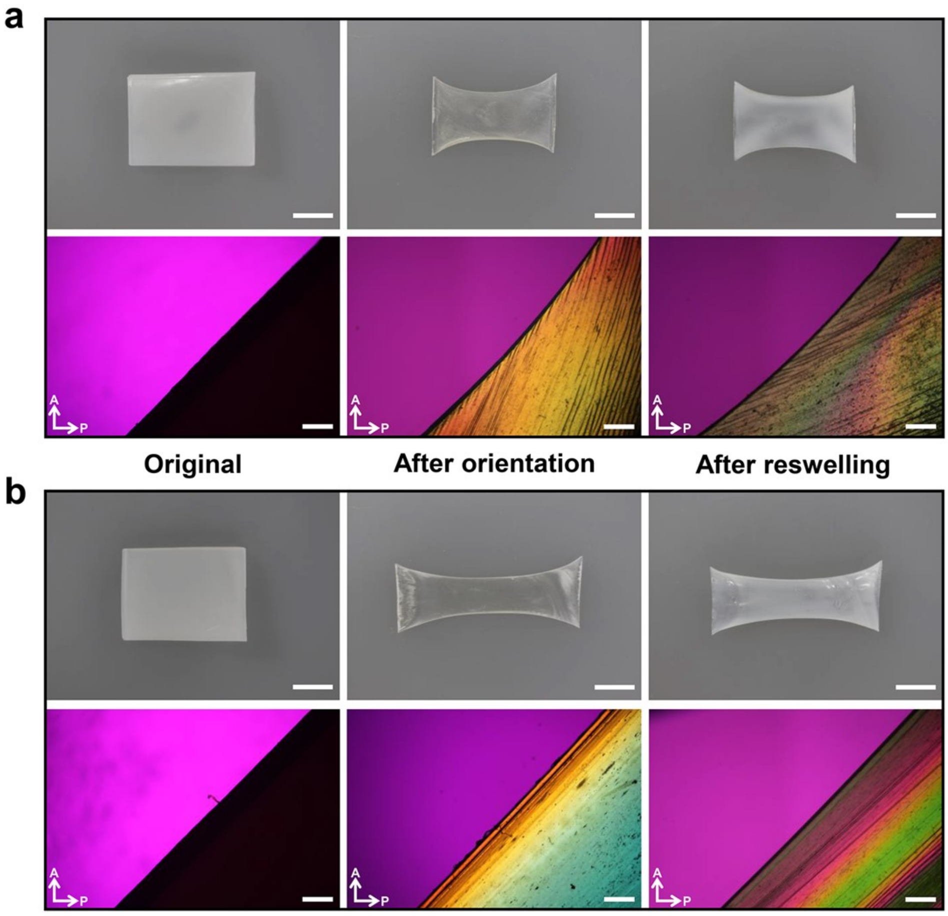

**Figure S3. Tunable anisotropy of the hybrid hydrogels by adjusting the pre-stretch ratio.** (a) The photographs and POM images of a PAAm/$Ca^{2+}$-Alg hybrid hydrogel that undergoes the orienting-reswelling process at a pre-stretch ratio of 0%. (b) The photographs and POM images of a PAAm/$Ca^{2+}$-Alg hybrid hydrogel that undergoes the orienting-reswelling process at a pre-stretch ratio of 50%. The two gels can both be oriented using the orienting-reswelling method, whereas they show different birefringence (**Figure 1e** in the manuscript) due to the different pre-stretch ratios. A: analyzer, P: polarizer. The scale bars in the photographs and POM images represent 10 mm and 200 μm, respectively.

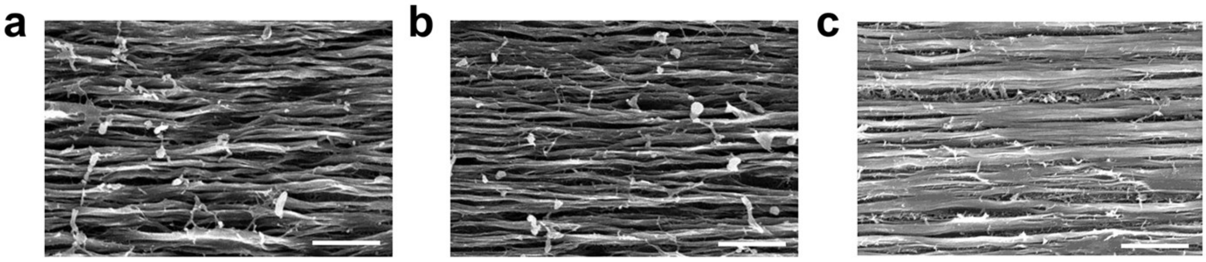

**Figure S4. The influence of the pre-stretch ratio ($\lambda_p$) on the microstructure of the hybrid gel after the orienting-reswelling process.** (a) The SEM image of the hybrid gel with $\lambda_p = 0\%$. (b) The SEM image of the hybrid gel with $\lambda_p = 50\%$. (c) The SEM image of the hybrid gel with $\lambda_p = 100\%$. The scale bars represent 20 μm.

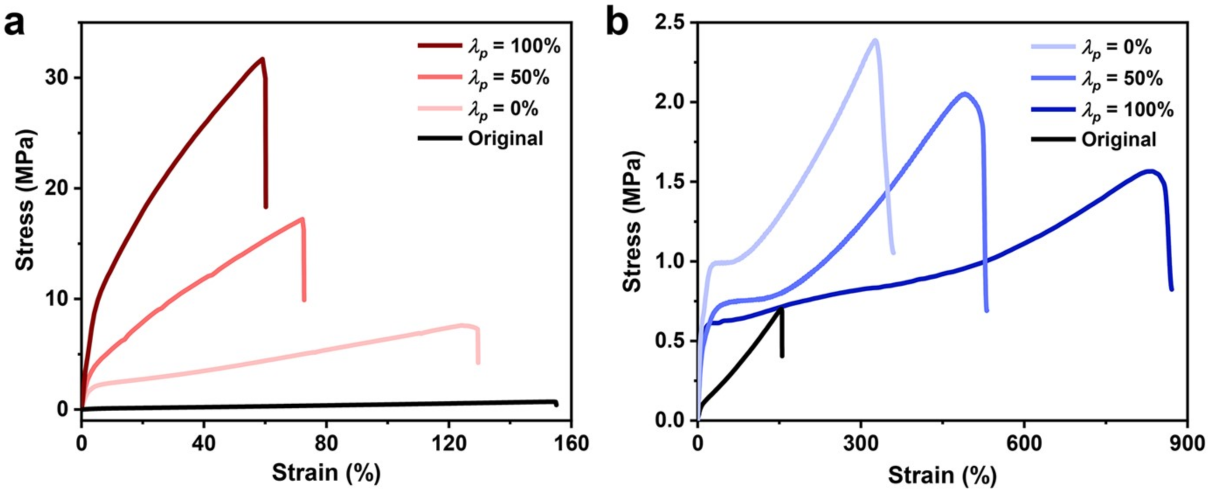

**Figure S5. Tunable anisotropic mechanical properties of the oriented hybrid gel by adjusting the pre-stretch ratio ($\lambda_p$), with the original non-oriented gel for comparison.** (a) The tensile stress-strain curves of the oriented hybrid gels with varied $\lambda_p$ parallel to the orientation. The stress-strain curve of the original non-oriented hybrid gel is also shown for comparison. (b) The tensile stress-strain curves of the oriented hybrid gels with varied $\lambda_p$ perpendicular to the orientation. The stress-strain curve of the original non-oriented hybrid gel is also shown for comparison.

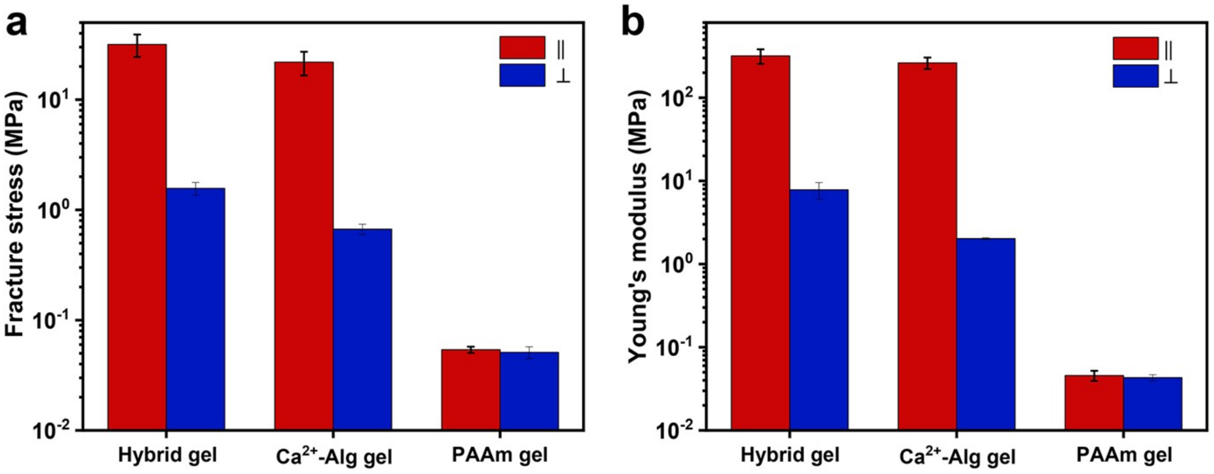

**Figure S6. Summarized anisotropic mechanical properties of the oriented hybrid gel ($\lambda_p = 100\%$), the Ca$^{2+}$-Alg gel, and the PAAm gel, respectively.** (a) The fracture stress of the three gels along and perpendicular to the orientation. (b) Young's modulus of the three gels along and perpendicular to the orientation. Both the oriented hybrid gel and the Ca$^{2+}$-Alg gel show mechanical anisotropy, while the PAAm gel shows isotropic mechanical properties.

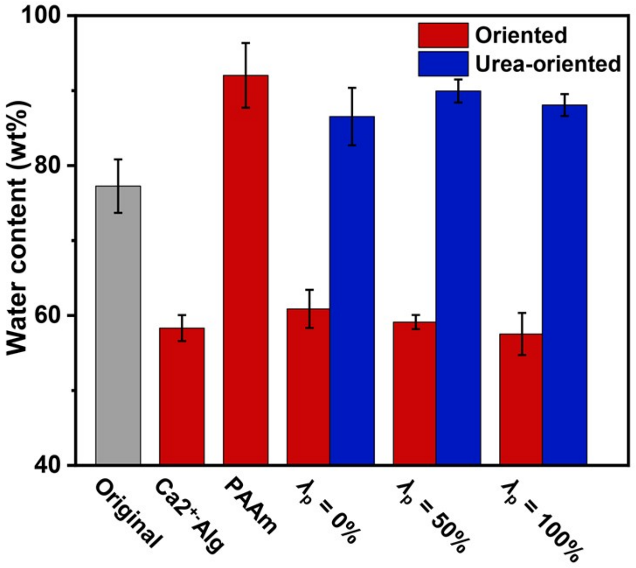

**Figure S7. The water content of the neat $Ca^{2+}$-Alg and PAAm gels after the orienting-reswelling process as well as the original, oriented, and urea-treated oriented hybrid hydrogels.** The original oriented hybrid gel has a water content that is higher than the neat $Ca^{2+}$-Alg gel and lower than the neat PAAm gel after the orienting-reswelling process. The hybrid gel possesses a decreased water content after the orienting-reswelling process. However, the water content significantly increases and even exceeds that of the original gel after urea treatment due to dramatic swelling of the gel.

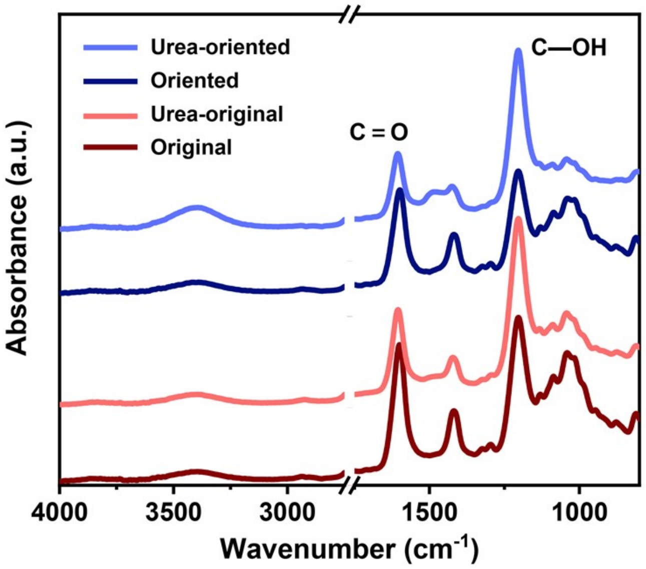

**Figure S8. FT-IR spectra (wavenumber from 4000 to 800 $cm^{-1}$) of the oriented ($\lambda_p = 100\%$) and original hybrid hydrogels before and after urea treatment, respectively.** The absorption peak at around 1600 $cm^{-1}$ is attributed to the asymmetric stretching vibration of the C=O group. The C—OH bond of the alginate shows an absorption peak at around 1200 $cm^{-1}$. The shift of the C=O peak is highlighted in **Figure 4c** to indicate the influence of urea treatment on supramolecular interactions in the hybrid gels.

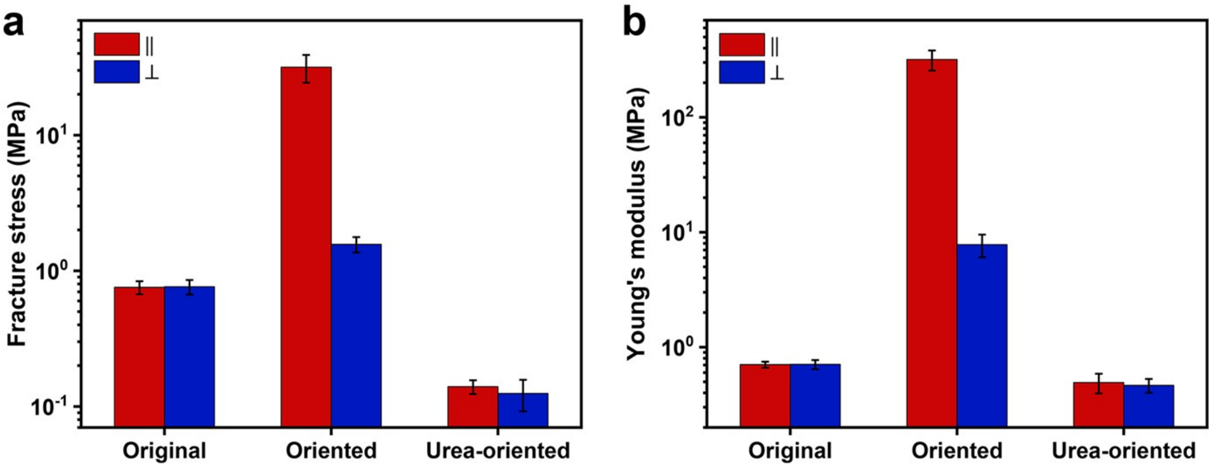

**Figure S9. Comparison of mechanical properties of the original, oriented, and urea-treated oriented hybrid hydrogels, respectively.** (a) The fracture stress of the original, oriented, and urea-treated oriented hybrid hydrogels parallel and perpendicular to the orientation, respectively. (b) The Young's modulus of the original, oriented, and urea-treated oriented hybrid hydrogels parallel and perpendicular to the orientation, respectively. The $\lambda_p$ of the oriented hybrid gel is 100%. The oriented hybrid gel shows clear mechanical anisotropy and much higher fracture stress and Young's modulus compared to the original and urea-treated oriented gels. The urea-treated oriented hybrid gel loses mechanical anisotropy and possesses even lower mechanical properties compared to the original hybrid gel, indicating the disappearance of the supramolecular interactions due to urea treatment.

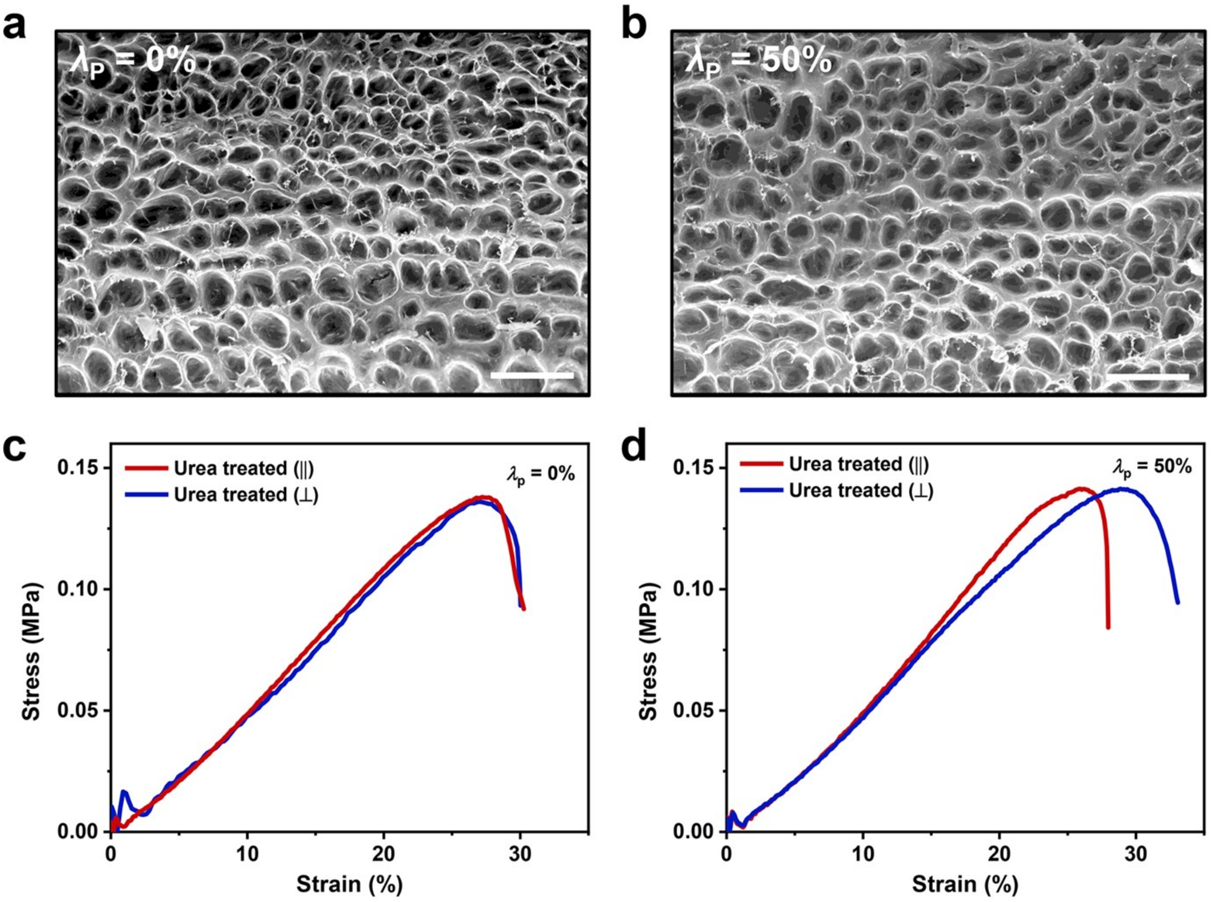

**Figure S10. The microstructures and mechanical properties of the oriented hybrid hydrogels with $\lambda_p$= 0% and 50% after urea treatment, respectively.** (a) The microstructure of the oriented hybrid hydrogel with $\lambda_p$= 0% after urea treatment. (b) The microstructure of the oriented hybrid hydrogel with $\lambda_p$= 50% after urea treatment. (c) Tensile stress-strain curves of the urea-treated oriented hybrid gel with $\lambda_p$= 0% parallel and perpendicular to orientation, respectively. (d) Tensile stress-strain curves of the urea-treated oriented hybrid gel with $\lambda_p$= 50% parallel and perpendicular to orientation, respectively. The scale bars represent 10 μm. The results show that the anisotropic structure of the oriented hybrid gels disappears due to the urea treatment. Meanwhile, the urea-treated oriented hydrogels no longer show anisotropic mechanical properties.

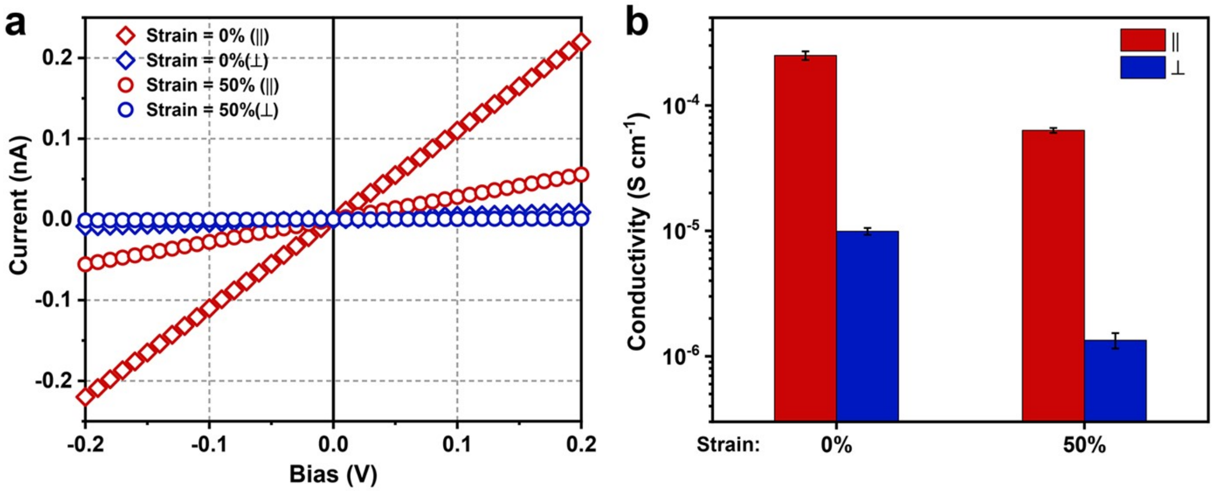

**Figure S11. The anisotropic ionic conductivity of the oriented hybrid gel ($\lambda_p$ = 100%, equilibrated in $10^{-5}$ M KCl solution) under or not under tension, respectively.** (a) I-V curves of the oriented hybrid gel along and perpendicular to the orientation at a strain of 0% and 50%, respectively. (b) The calculated conductivity of the oriented hybrid gel along and perpendicular to the orientation at a strain of 0% and 50%, respectively.

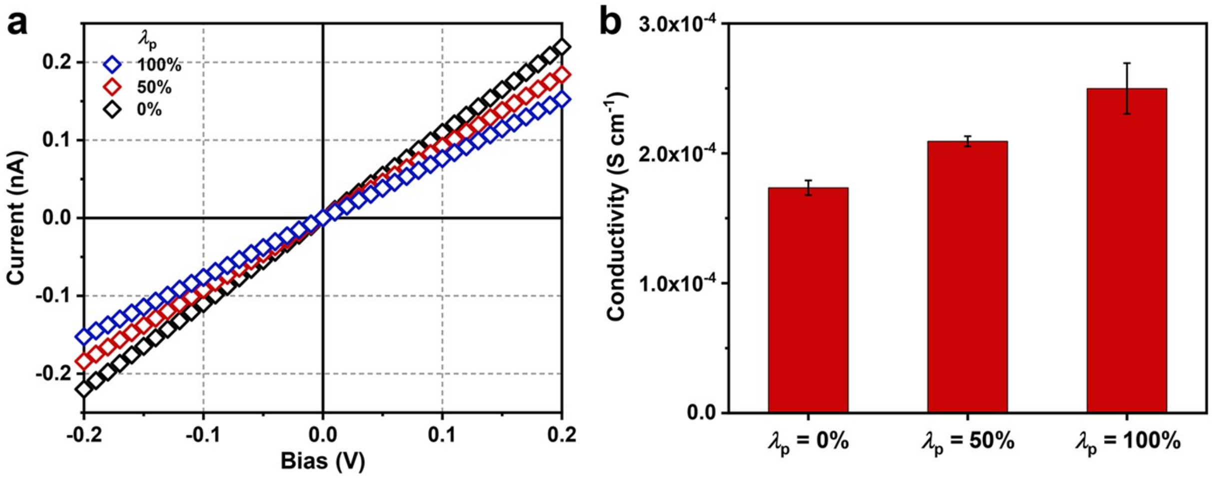

**Figure S12. The influence of the pre-stretch ratio on the ionic conductive of the oriented hybrid gel ($\lambda_p$ = 100%, equilibrated in $10^{-5}$ M KCl solution).** (a) I-V curves of the oriented hybrid gels with varied $\lambda_p$ along the orientation. (b) The calculated ionic conductivity of the oriented hybrid gels with varied $\lambda_p$ along the orientation.